JACS
JOURNAL OF THE AMERICAN CHEMICAL SOCIETY

Communication

pubs.acs.org/JACS

# Interrogating Near-Infrared Electrogenerated Chemiluminescence of $Au_{25}(SC_2H_4Ph)_{18}^+$ Clusters

Kalen N. Swanick, Mahdi Hesari, Mark S. Workentin, and Zhifeng Ding*

Department of Chemistry and Centre for Advanced Materials and Biomaterials, The University of Western Ontario, London, Ontario, Canada N6A 5B7

Supporting Information

**ABSTRACT:** The electrochemistry, near-infrared photoluminescence (NIR-PL) spectroscopy, and electrogenerated chemiluminescence (ECL) of $Au_{25}(SC_2H_4Ph)_{18}^+$-$C_6F_5CO_2^-$ ($Au_{25}^+$) clusters were investigated. For the first time, NIR-ECL emission was observed in both annihilation and coreactant paths. Our newly developed spooling spectroscopy was employed during the ECL evolution and devolution processes along with explicit NIR-PL spectroscopy to elucidate light generation mechanisms. It was discovered that the electronic relaxation of the $Au_{25}^-$ excited state to the ground state plays a key role in giving off ECL at 893 nm, while intermediate, strong, and weak NIR-PL emissions at 719/820, 857, and 1080 nm can be attributed to the excited states higher than the HOMO-LUMO gap, across the HOMO-LUMO gap, and of semi-rings, respectively.

The optical properties of nanostructures such as silicon nanocrystals (NCs),[1] carbon quantum dots,[2] and gold nanoparticles (NPs)[3] are attractive to many researchers because of their potential applications.[4] Among a variety of gold NPs, $Au_{25}L_{18}$ clusters have been the focus of recent investigations due to their molecule-like (1.1 nm in diameter) behavior, monodispersed synthesis protocols,[5] and unique optical,[6] electrochemical,[7] and structural portfolio.[8] A $Au_{25}$ cluster consists of an icosahedral $Au_{13}$ core and six semi-rings containing -Au-S-Au-S-.[6g,9] Murray et al.[3] and Jin et al.[10] pioneered studies exploring the various properties of $Au_{25}$, for instance, observing the difference in photoluminescence (PL) by changing the combination of protecting ligands and electropositivity.[11] These studies showed that the origins of the clusters' optical properties are dependent on the charge and protecting ligand's functionalities.[10a] Zhu et al. and Chen et al. demonstrated that Au clusters protected by bovine serum albumin (BSA) can also be utilized in analytical detection methods based on spectroscopic properties of the Au-BSA cluster.[12] Of the stable charged states of $Au_{25}L_{18}^z$ ($z = -1$, 0, and +1), the −1 form is the most studied, although recent synthetic protocols have allowed the isolation and investigation of the 0 and +1 states. The different charged states induce various properties on the gold clusters that have been probed by $^1$H NMR,[13] PL,[10a] and electron paramagnetic resonance spectroscopy.[14]

Electrogenerated chemiluminescence (ECL) is the process in which electrogenerated radicals form excited species emitting light without the need of an external light source.[15] Advantages of ECL include simultaneous generation of radical cations and anions and the control of electrode potentials that drive light emission processes. ECL has great potential in biological applications such as detection in immunoassays, food and water testing, trace metal determination, sensors, and biomolecules.[15] Our motivation is to explore ECL of various compounds[2b,c,16] toward applications in biosensors and bioanalytical chemistry.

Herein, we report the ECL of $Au_{25}$ in the near-infrared (NIR) region by means of spooling spectroscopy to gain insight into ECL mechanisms during potentiodynamic processes. Previously, ECL studies of $Au_{25}$ clusters have been conducted in aqueous solution and resulted in very weak ECL only in the visible region.[12] Generating NIR-ECL light is especially important for bioimaging applications, but there are few reports on NIR-ECL[17] and no reports on NIR-ECL of Au clusters. Furthermore, the fact that $Au_{25}$ clusters have at least three excited states corresponding to their oxidation states gives a unique opportunity to interrogate spectroelectrochemical properties correlating to their structures.[13,14,18] For the first time, NIR-ECL of the $Au_{25}$ has been observed, and mechanisms for the NIR emission have been explored. The correlation of the $Au_{25}^+$ structure, revealed by DFT calculation in literature, electrochemistry, and UV−vis and PL spectroscopy to the ECL emission processes is presented.

$Au_{25}(SC_2H_4Ph)_{18}^+C_6F_5CO_2^-$ clusters, referred to as $Au_{25}^+$, were synthesized and purified utilizing established procedures reported by Maran et al. (see SI).[13a,19] The electrochemistry of dilute 0.67 mg/mL $Au_{25}^+$ cluster electrolyte solutions was investigated by cyclic voltammetry (CV) and differential pulse voltammetry (DPV), and representative traces are shown in Figure S11A[16a,b] and Figure 1A, respectively. DPV better displays the redox behavior at this low concentration of $Au_{25}^+$ (required for the ECL study) due to suppression of the background current. During cathodic scanning (red curve, Figure 1A) of the applied potential, two quasi-reversible reduction waves are observed with half-wave potentials[15b] of 0.244 and −0.008 V. These correspond to the $Au_{25}^+$ clusters being reduced consecutively to $Au_{25}^0$ and then $Au_{25}^-$ (eqs 1 and 2). The energy difference to convert $Au_{25}^+$ to $Au_{25}^-$ via the two successive electrons is 0.252 eV. $Au_{25}^-$ displays similar CV and DPV with a similar energy value to remove two successive electrons.[10a,18a] At more negative potentials there is a broad, irreversible reduction wave with an estimated half-wave potential of −0.990 V corresponding to the further reduction of $Au_{25}^-$ to $Au_{25}^{2-}$ (eq

**Received:** June 21, 2012
**Published:** August 28, 2012





dx.doi.org/10.1021/ja306047u | J. Am. Chem. Soc. 2012, 134, 15205−15208

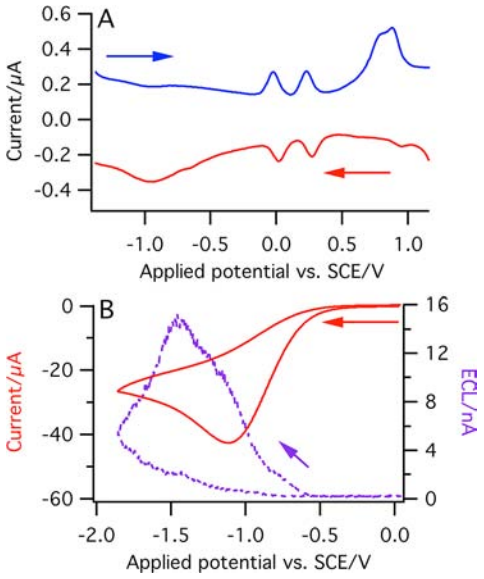


**Figure 1.** (A) Differential pulse voltammograms of 0.67 mg/mL $Au_{25}^{+}$ clusters in 1:1 benzene/acetonitrile solution, with 0.1 M tetra-*n*-butylammonium perchlorate as supporting electrolyte. (B) Cyclic voltammogram and ECL-voltage curve for a $Au_{25}^{+}$ cluster solution with 5 mM benzoyl peroxide.

3). This reduction injects an electron into the LUMO, making $Au_{25}^{2-}$ less stable. The anodic scan (blue curve, Figure 1A) shows the two well-defined waves corresponding to the reverse of eqs 1 and 2 and, at potentials more positive than 0.510 V, two more irreversible reactions corresponding to the oxidation of $Au_{25}^{+}$ to $Au_{25}^{2+}$ and $Au_{25}^{3+}$ (eqs 4 and 5). These half-wave potentials were roughly estimated to be 0.825 and 0.900 V, respectively. Note that $Au_{25}^{2+}$ is known to be unstable,[20] leading to a smaller current for the following oxidation.

$$Au_{25}^{+} + e^{-} \rightarrow Au_{25}^{0} \quad (1)$$

$$Au_{25}^{0} + e^{-} \rightarrow Au_{25}^{-} \quad (2)$$

$$Au_{25}^{-} + e^{-} \rightarrow Au_{25}^{2-} \quad (3)$$

$$Au_{25}^{+} \rightarrow Au_{25}^{2+} + e^{-} \quad (4)$$

$$Au_{25}^{2+} \rightarrow Au_{25}^{3+} + e^{-} \quad (5)$$

For $Au_{25}^{+}$ the potential difference between the first oxidation (eq 4) and third reduction (eq 3) peaks gives an estimation on the HOMO-LUMO energy gap of 1.558 eV after charging correction.[18a] This is a very rough estimation because of the irreversibility of the reduction of $Au_{25}^{-}$ to $Au_{25}^{2-}$ (eq 3) and possible complexity of side reactions like its analogues, $Au_{38}$ and $Au_{147}$ clusters, that shifts the peak potential of the third reduction from the true standard potential.[21] This electrochemical energy gap corresponds well to the observed 1.538 eV optical absorption onset of $Au_{25}^{+}$ in $CH_2Cl_2$ (Figure S5) and is close to that (1.48 eV) calculated by DFT for $Au_{25}^{-}$, which has paired electrons in all three HOMOs.[22]

The ECL of the solution above was measured upon continuous alternative electrochemical oxidation and reduction between the potentials defined by eqs 3 and 4. The $Au_{25}^{+}$ solution exhibited very weak ECL via this annihilation path[15b,c,16a,b,23] (Figure S11B), where electrogenerated $Au_{25}^{2+}$ and $Au_{25}^{2-}$ react and $Au_{25}^{-}$* excited state is produced, emitting light upon relaxation to the ground state (eqs 6 and 7). It is found that $Au_{25}^{2-}$ is more stable than $Au_{25}^{2+}$ since ECL can only be observed in the anodic potential region. No ECL spectrum was obtained due to low intensity caused by the instability of the dication and dianion.[20]

$$Au_{25}^{2-} + Au_{25}^{2+} \rightarrow Au_{25}^{-}* + Au_{25}^{+} \quad (6)$$

$$Au_{25}^{-}* \rightarrow Au_{25}^{-} + h\nu \quad (7)$$

Figure 1B presents a CV trace along with the corresponding ECL-voltage curve of a $Au_{25}^{+}$ solution with 5 mM benzoyl peroxide (BPO, $(C_6H_5CO)_2O_2$), a common cathodic ECL coreactant.[15c,24] ECL has an onset potential of −0.560 V, at which BPO was reduced to $BPO^{-\bullet}$ (eq 8)[16a,b,24a,b] and the $Au_{25}^{+}$ underwent a two-step reduction reaction to $Au_{25}^{-}$ as in eqs 1 and 2. In the diffusion layer containing the above two species, a strong oxidizing intermediate radical $C_6H_5CO_2^{\bullet}$ was generated via decomposition of $BPO^{-\bullet}$ (eq 9), which accepts one electron from $Au_{25}^{-}$ and transforms it to $Au_{25}^{0}$ (eq 10). The $Au_{25}^{-}$* excited state was generated by transferring one electron from $BPO^{-\bullet}$ to the LUMO of $Au_{25}^{0}$ (eq 11),[16b] which emitted light upon relaxation to the ground state (eq 7). The ECL-voltage curve shows a slight maximum at −0.793 V. This ECL mechanism is very similar to that of a molecular luminophore with BPO as coreactant prior to reducing the luminophore.[16b]

$$BPO + e^{-} \rightarrow BPO^{-\bullet} \quad (8)$$

$$BPO^{-\bullet} \rightarrow C_6H_5CO_2^{\bullet} + C_6H_5CO_2^{-} \quad (9)$$

$$C_6H_5CO_2^{\bullet} + Au_{25}^{-} \rightarrow Au_{25}^{0} + C_6H_5CO_2^{-} \quad (10)$$

$$Au_{25}^{0} + BPO^{-\bullet} \rightarrow Au_{25}^{-}* + BPO \quad (11)$$

The ECL intensity in the BPO coreactant system increased dramatically when the applied potential was scanned to more negative potentials. As described above, $Au_{25}^{2-}$ is the dominant species in the vicinity of the electrode biased more negative than −0.980 V. $Au_{25}^{-}$* was generated in this potential region by the reaction of $Au_{25}^{2-}$ either with $Au_{25}^{0}$ (eq 12) or $C_6H_5CO_2^{\bullet}$ in the diffusion layer (eq 13) or with $Au_{25}^{+}$ in the bulk solution (eq 14). ECL intensity reached the highest at −1.458 V.

$$Au_{25}^{0} + Au_{25}^{2-} \rightarrow Au_{25}^{-}* + Au_{25}^{-} \quad (12)$$

$$C_6H_5CO_2^{\bullet} + Au_{25}^{2-} \rightarrow Au_{25}^{-}* + C_6H_5CO_2^{-} \quad (13)$$

$$Au_{25}^{+} + Au_{25}^{2-} \rightarrow Au_{25}^{-}* + Au_{25}^{0} \quad (14)$$

The strong oxidizing intermediate radical, $C_6H_5CO_2^{\bullet}$, may persist in solution long enough to combine with the reduced forms of the clusters, also generating the excited species in solution. While the BPO coreactant systems is complicated,[24c] the presence of multiple oxidation states of the cluster adds even more complexity, and additional ECL mechanisms can be proposed based on the possible combinations. It is noteworthy that no ECL was observed in a BPO solution containing no $Au_{25}^{0}$ (Figure S12) in the same potential window.

The increased ECL intensity using a coreactant allowed the acquisition of ECL spectra. Figure 2A presents ECL spectra acquired on solutions containing $Au_{25}^{+}$ clusters with BPO with a time interval of 1 s during potentiodynamic scanning from 0.040 to −1.860 V and back to 0.040 V. Figure S9A shows the voltammogram at a scan rate of 0.1 V/s during this spectroelectrochemical measurement, which is very similar to


dx.doi.org/10.1021/ja306047u | J. Am. Chem. Soc. 2012, 134, 15205−15208

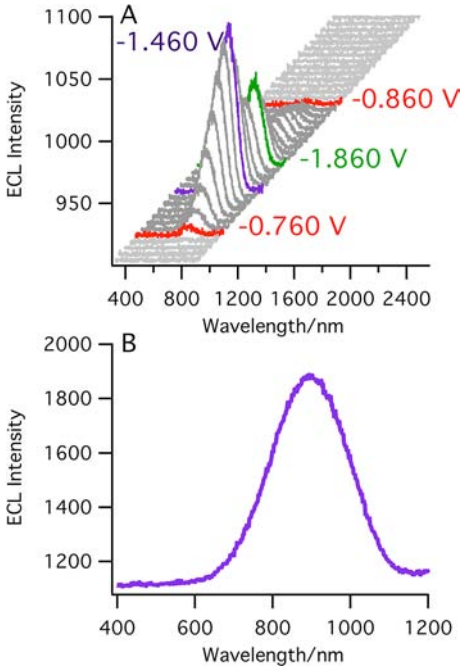


**Figure 2.** (A) Spooled ECL spectra of $Au_{25}^{+}$ clusters with BPO during one cycle of the applied potential from 0.04 to −1.86 V then back to 0.04 V. Each spectrum was acquired for 1 s using an iDUS NIR CCD camera cooled to −75 °C. (B) Typical accumulated ECL spectrum of the same coreactant solution collected over 80 s, two cycles of potential scanning between 0.04 and −1.86 V at a scan rate of 0.1 V/s.

that in Figure 1B. The spectroelectrochemistry was carried out by means of our newly developed spooling spectroscopy for ECL. Briefly, the ECL cell was placed into a holder attached to an Acton spectrograph with an Andor NIR CCD camera cooled to −75 °C, and ECL processes were driven by the potential scanning at 0.1 V/s in the range between 0.040 and −1.860 V, with a spectrum recorded every 100 mV, which is equivalent to 1 s. The spectra in Figure 2A track the evolution and devolution of the ECL emission and give insight into the ECL mechanisms. As was observed in the ECL-voltage curve shown in Figure 1B, a pronounced ECL spectrum (Figure 2A, red spectrum) was obtained at −0.760 V on the forward scan. The peak wavelength was determined to be 893 nm (1.390 eV), very close to the HOMO-LUMO energy gap of $Au_{25}^{+}$ estimated above by electrochemistry and UV−vis spectroscopy and calculated for $Au_{25}^{-}$ by DFT.[22] The ECL intensity increased as the potential was made more negative up to −1.460 V, while the ECL peak wavelength remained constant at 893 nm (purple in Figure 2A). As the applied potential became even more negative, the ECL peak intensity decreased due to the concentration depletion of the clusters as well as BPO. This is illustrated in Figure 2A between −1.460 (purple spectrum) and −1.860 V (green spectrum). On the reverse potential scan from −1.860 to 0.040 V, the ECL spectra devolve. Because the ECL peak wavelength remains constant at 893 nm throughout the potential window, this is indicative of only one excited state being involved. This is further exemplified in Figure S9, where the spectra over two potential cycles are shown and the ECL peak wavelength remains the same. The above observations support very well the proposed ECL mechanisms as expressed by eqs 6−12 and agree with the ECL-voltage curve in Figure 1B. Furthermore, an ECL spectrum accumulated for 80 s was also collected by scanning the potential between 0.04 and −1.86 V at a scan rate of 0.1 V/s. The acquired spectrum displays a maximum wavelength of 893 nm as well (Figure 2B), which confirms that only one excited state is involved in the ECL process.

It is informative to compare the ECL spectra (Figure 2)with PL spectra measured on a solution of $Au_{25}^{-}$ (Figure 3) in order to

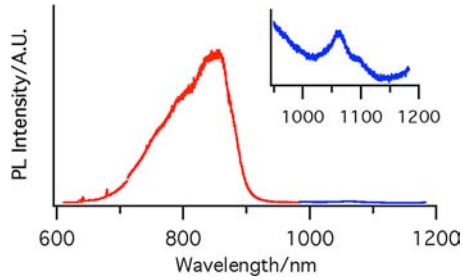


**Figure 3.** Photoluminescence of a $Au_{25}^{-}$ 1:1 benzene/acetonitrile solution using an iDus 401 CCD camera between 633 and 1200 nm upon excitation at 633 nm.

confirm the identity of the excited state involved in the ECL processes. The PL spectra were measured on the same spectrograph and CCD camera set used for the ECL measurements to exclude any ambiguities about the PL spectrum of the clusters measured previously on different instruments/detectors.[10,11] Our confocal setup covers the entire spectral range (630−1180 nm) of interest and a peak response quantum efficiency of 95% at 800 nm (see SI for the instrument specification). Figure 3 depicts a typical PL spectrum of the $Au_{25}^{-}$ cluster solution, showing two luminescence shoulders at 719 (1.72 eV) and 820 nm (1.51 eV), as reported by the Jin group[10] and similar to the Au cluster investigated by El-Sayed and Whetten.[25] Also observed was a strong peak at 857 nm (1.45 eV), as well as a weak one at 1080 nm (1.15 eV, inset in Figure 3), as described by the Murray group.[11] The only difference between our results and those reported earlier is in the intensity pattern due to differences in the detector response efficiencies in the different setups being compared (Figure S10). The most interesting luminescence peak is the strongest one at 857 nm, which can be assigned to the excited-state luminescence emission with energy higher than that from a relaxed excited state across the HOMO-LUMO gap at 1.349 eV.[25] The other two shoulders may be the excited states populated from the electron promotion from HOMO-1 to LUMO or HOMO to LUMO+1. The weak luminescence peak can be assigned to semi-ring states, namely phosphorescence emission due to the transition from a triplet excited state to the ground state, as in the case of Au clusters reported by Moran and Murray with femtosecond spectroscopy[6d] and by the Murray group NIR-PL spectroscopy.[18a,25]

Our spooling $Au_{25}^{+}$ ECL spectra clearly identify the excited state in the whole ECL process to be $Au_{25}^{-*}$ across the HOMO-LUMO gap, giving an emission peaked at 893 nm (1.390 eV). This agrees very well with our elucidated ECL mechanisms above. From a thermodynamics point of view, the excited state in ECL was generated directly from radical reactions without the nonradioactive relaxation of excited states in PL processes. Our ECL and PL emission are in agreement with the observations from PL spectra of $Au_{25}^{-}$ solution. Based on the atomic contributions to the HOMOs that are essentially superatom P orbitals and LUMOs that comprise mainly D orbitals from the DFT calculation[22] and magnetic circular dichroism spectroscopy,[18b] the ECL emission observed is likely due to the radioactive electronic relaxation from the LUMOs to HOMOs.


dx.doi.org/10.1021/ja306047u | J. Am. Chem. Soc. 2012, 134, 15205−15208

The above observation on ECL of $Au_{25}$ clusters is very different from that on ECL of silicon NCs, which depended more sensitively on surface chemistry and the presence of rich surface states,[1] as previously reported by Ding et al. While thiophenolate ligands having more electron-withdrawing substituents enhance the PL of semi-ring states in $Au_{25}^-$ clusters,[11] ECL is favored in the electronic relaxation across the HOMO-LUMO gap. This is probably due to the activity of the cluster icosahedral $Au_{13}$ core incompletely covered by protecting ligand complexes or six staple-shaped motifs (-S-Au-S-Au-S-).[14,26] It is plausible that semi-ring state emission observed in PL plays a minor role in ECL, possibly because its intensity is not as high as that of surface states in larger NCs.

In summary, this work unambiguously demonstrates that NIR-ECL of $Au_{25}$ can be observed in annihilation of electrogenerated $Au_{25}^{2+}$ and $Au_{25}^{2-}$ species and enhanced in the path of coreactant system with BPO. The light emission was explicitly elucidated as being due to the electronic relaxation of the $Au_{25}^{-}$* excited state to the ground state across HOMO-LUMO gap by means of electrochemistry, PL spectroscopy, and our newly developed spooling spectroscopy during the ECL evolution and devolution.

## ■ ASSOCIATED CONTENT

### Supporting Information

Experimental procedures, spectra, quantum yield calculation, ECL-voltage curves, and cyclic voltammograms. This material is available free of charge via the Internet at http://pubs.acs.org.

## ■ AUTHOR INFORMATION


### Corresponding Author

zfding@uwo.ca


### Notes

The authors declare no competing financial interest.

## ■ ACKNOWLEDGMENTS

This research is supported by NSERC, OCE, CFI/OIT, PREA, and The University of Western Ontario. We acknowledge our Electronic Shop and ChemBio Store for the quality service.

## ■ REFERENCES


(1) Ding, Z.; Quinn, B. M.; Haram, S. K.; Pell, L. E.; Korgel, B. A.; Bard, A. J. *Science* **2002**, *296*, 1293.

(2) (a) Bourlinos, A. B.; Zbořil, R.; Petr, J.; Bakandritsos, A.; Krysmann, M.; Giannelis, E. P. *Chem. Mater.* **2011**, *24*, 6. (b) Zhou, J.; Booker, C.; Li, R.; Zhou, X.; Sham, T.-K.; Sun, X.; Ding, Z. *J. Am. Chem. Soc.* **2007**, *129*, 744. (c) Zhou, J.; Booker, C.; Li, R.; Sun, X.; Sham, T.-K.; Ding, Z. *Chem. Phys. Lett.* **2010**, *493*, 296.

(3) Wang, G.; Huang, T.; Murray, R. W.; Menard, L.; Nuzzo, R. G. *J. Am. Chem. Soc.* **2005**, *127*, 812.

(4) (a) Wu, Z.; Wang, M.; Yang, J.; Zheng, X.; Cai, W.; Meng, G.; Qian, H.; Wang, H.; Jin, R. *Small* **2012**, *8*, 2028. (b) Ghosh Chaudhuri, R.; Paria, S. *Chem. Rev.* **2012**, *112*, 2373. (c) Lu, Y.; Chen, W. *Chem. Soc. Rev.* **2012**, *41*, 3594. (d) Murray, R. W. *Chem. Rev.* **2008**, *108*, 2688.

(5) (a) Wu, Z.; Suhan, J.; Jin, R. *J. Mater. Chem.* **2009**, *19*, 622. (b) Dharmaratne, A. C.; Krick, T.; Dass, A. *J. Am. Chem. Soc.* **2009**, *131*, 13604.

(6) (a) Devadas, M. S.; Kim, J.; Sinn, E.; Lee, D.; Goodson, T.; Ramakrishna, G. *J. Phys. Chem. C* **2010**, *114*, 22417. (b) Sakanaga, I.; Inada, M.; Saitoh, T.; Kawasaki, H.; Iwasaki, Y.; Yamada, T.; Umezu, I.; Sugimura, A. *Appl. Phys. Exp.* **2011**, *4*, 095001. (c) Devadas, M. S.; Bairu, S.; Qian, H.; Sinn, E.; Jin, R.; Ramakrishna, G. *J. Phys. Chem. Lett.* **2011**, *2*, 2752. (d) Miller, S. A.; Womick, J. M.; Parker, J. F.; Murray, R. W.; Moran, A. M. *J. Phys. Chem. C* **2009**, *113*, 9440. (e) Qian, H.; Sfeir, Y.; Jin, M. *J. Phys. Chem. C* **2010**, *114*, 19935. (f) Parker, J. F.; Fields-Zinna, C. A.; Murray, R. W. *Acc. Chem. Res.* **2010**, *43*, 1289. (g) Zhu, M.; Aikens, C. M.; Hollander, F. J.; Schatz, G. C.; Jin, R. *J. Am. Chem. Soc.* **2008**, *130*, 5883.

(7) (a) Garcia-Raya, D.; Madueno, R.; Blazquez, M.; Pineda, T. *J. Phys. Chem. C* **2009**, *113*, 8756. (b) Kumar, S. S.; Kwak, K.; Lee, D. *Electroanalysis* **2011**, *23*, 2116.

(8) (a) MacDonald, M. A.; Chevrier, D. M.; Zhang, P.; Qian, H.; Jin, R. *J. Phys. Chem. C* **2011**, *115*, 15282. (b) Perera, N. V.; Isley, W.; Maran, F.; Gascon, J. A. *J. Phys. Chem. C* **2010**, *114*, 16043. (c) Akola, J.; Kacprzak, K. A.; Lopez-Acevedo, O.; Walter, M.; Gronbeck, H.; Hakkinen, H. *J. Phys. Chem. C* **2010**, *114*, 15986.

(9) (a) Zhu, M.; Eckenhoff, W. T.; Pintauer, T.; Jin, R. *J. Phys. Chem. C* **2008**, *112*, 14221. (b) Heaven, M. W.; Dass, A.; White, P. S.; Holt, K. M.; Murray, R. W. *J. Am. Chem. Soc.* **2008**, *130*, 3754.

(10) (a) Wu, Z.; Jin, R. *Nano Lett.* **2010**, *10*, 2568. (b) Qian, H.; Zhu, M.; Wu, Z.; Jin, R. *Acc. Chem. Res.* **2012**, DOI: 10.1021/ar200331z.

(11) Wang, G.; Guo, R.; Kalyuzhny, G.; Choi, J.-P.; Murray, R. W. *J. Phys. Chem. B* **2006**, *110*, 20282.

(12) (a) Fang, Y.-M.; Song, J.; Li, J.; Wang, Y.-W.; Yang, H.-H.; Sun, J.-J.; Chen, G.-N. *Chem. Commun.* **2011**, *47*, 2369. (b) Li, L.; Liu, H.; Shen, Y.; Zhang, J.; Zhu, J.-J. *Anal. Chem.* **2011**, *83*, 661.

(13) (a) Venzo, A.; Antonello, S.; Gascon, J. A.; Guryanov, I.; Leapman, R. D.; Perera, N. V.; Sousa, A.; Zamuner, M.; Zanella, A.; Maran, F. *Anal. Chem.* **2011**, *83*, 6355. (b) Liu, Z.; Zhu, M.; Meng, X.; Xu, G.; Jin, R. *J. Phys. Chem. Lett.* **2011**, *2*, 2104.

(14) Zhu, M.; Aikens, C. M.; Hendrich, M. P.; Gupta, R.; Qian, H.; Schatz, G. C.; Jin, R. *J. Am. Chem. Soc.* **2009**, *131*, 2490.

(15) (a) Miao, W. *Chem. Rev.* **2008**, *108*, 2506. (b) Bard, A. J.; Faulkner, L. R. *Electrochemical Methods, Fundamentals and Applications*; 2nd ed.; Wiley: New York, 2001. (c) Bard, A. J. *Electrogenerated Chemiluminescence*; Marcel Dekker: New York, 2004.

(16) (a) Swanick, K. N.; Dodd, D. W.; Price, J. T.; Brazeau, A. L.; Jones, N. D.; Hudson, R. H. E.; Ding, Z. *Phys. Chem. Chem. Phys.* **2011**, *13*, 17405. (b) Swanick, K. N.; Ladouceur, S.; Zysman-Colman, E.; Ding, Z. *Chem. Commun.* **2012**, *48*, 3179. (c) Booker, C.; Wang, X.; Haroun, S.; Zhou, J.; Jennings, M.; Pagenkopf, B. L.; Ding, Z. *Angew. Chem., Int. Ed.* **2008**, *47*, 7731.

(17) (a) Liang, G.; Shen, L.; Zou, G.; Zhang, X. *Chem. Eur. J.* **2011**, *17*, 10213. (b) Lee, S. K.; Richter, M. M.; Strekowski, L.; Bard, A. J. *Anal. Chem.* **1997**, *69*, 4126.

(18) (a) Lee, D.; Donkers, R. L.; Wang, G.; Harper, A. S.; Murray, R. W. *J. Am. Chem. Soc.* **2004**, *126*, 6193. (b) Yao, H. *J. Phys. Chem. Lett.* **2012**, *3*, 1701.

(19) Antonello, S.; Hesari, M.; Polo, F.; Maran, F. *Nanoscale* **2012**, *4*, 5333.

(20) Antonello, S.; Holm, A. H.; Instuli, E.; Maran, F. *J. Am. Chem. Soc.* **2007**, *129*, 9836.

(21) (a) Quinn, B. M.; Kontturi, K. *J. Am. Chem. Soc.* **2004**, *126*, 7168. (b) Toikkanen, O.; Ruiz, V.; Ronnholm, G.; Kalkkinen, N.; Liljeroth, P.; Quinn, B. M. *J. Am. Chem. Soc.* **2008**, *130*, 11049.

(22) Aikens, C. M. *J. Phys. Chem. C* **2008**, *112*, 19797.

(23) Bard, A. J.; Faulkner, L. R. In *Electroanalytical Chemistry*; Bard, A. J., Ed.; Dekker: New York, 1977; Vol. *10*, pp 1−95.

(24) (a) Choi, J.-P.; Wong, K.-T.; Chen, Y.-M.; Yu, J.-K.; Chou, P.-T.; Bard, A. J. *J. Phys. Chem. B* **2003**, *107*, 14407. (b) Lai, R. Y.; Fleming, J. J.; Merner, B. L.; Vermeij, R. J.; Bodwell, G. J.; Bard, A. J. *J. Phys. Chem. A* **2004**, *108*, 376. (c) Rosenthal, J.; Nepomnyashchii, A. B.; Kozhukh, J.; Bard, A. J.; Lippard, S. J. *J. Phys. Chem. C* **2011**, *115*, 17175.

(25) Link, S.; Beeby, A.; FitzGerald, S.; El-Sayed, M. A.; Schaaff, T. G.; Whetten, R. L. *J. Phys. Chem. B* **2002**, *106*, 3410.

(26) Akola, J.; Walter, M.; Whetten, R. L.; Häkkinen, H.; Grönbeck, H. *J. Am. Chem. Soc.* **2008**, *130*, 3756.